micro

MDPI

Article

Structural Inhomogeneities and Nonlinear Phenomena in Charge Transfer under Cold Field Emission in Individual Closed Carbon Nanotubes

S. V. von Gratowski [1,*], Z. Ya. Kosakovskaya [1,†], V. V. Koledov [1], V. G. Shavrov [1], A. M. Smolovich [1], A. P. Orlov [1], R. N. Denisjuk [1], Cong Wang [2] and Junge Liang [3]

1 Kotel'nikov Institute of Radioengineering and Electronics Russian Academy of Sciences, 11-7 Mokhovaya, 125009 Moscow, Russia; victor_koledov@mail.ru (V.V.K.); shavrov@cplire.ru (V.G.S.); papa@petersmol.ru (A.M.S.); ro-d@yandex.ru (R.N.D.)
2 Harbin Institute of Technology, 92 West Dazhi Street, Nan Gang District, Harbin 150001, China; kevinwang@hit.edu.cn
3 Department of Electronic Engineering, Engineering Research Center of IoT Technology Applications, Jiangnan University, Lihu Road 1800, Wuxi 214000, China; jgliang@jiangnan.edu.cn
* Correspondence: svetlana.gratowski@yandex.ru
† Z. Ya. Kosakovskaya made a great contribution to the research and creation of this article but deceased.

Abstract: The structure and phenomena arising from charge transfer in cold field emission mode in a single closed carbon nanotube (CNT) under cold field emission conditions are studied. Inhomogeneities of the structure of CNT in the form of two types of superlattices are found by studying microphotographs obtained by AFM, SEM, and TEM. The features of charge transfer in a quasi-one-dimensional carbon nanotube emitter with a small gap between the anode and cathode are studied under conditions of low-voltage field emission. It is established that the I-V characteristics reveal voltage thresholds and resonant peaks, which are associated with the opening of conduction channels in the region of van Hove singularities. In the region of peaks in the I-V characteristics, the emission current exceeds the one calculated using the Fowler–Nordheim (F-N) function by one to three orders of magnitude. The I-V characteristic is not that the curve straightens in F-N coordinates. It is found that the peaks in the I-V characteristics have distinct regions of negative differential conductivity.

Keywords: carbon nanotubes (CNTs); cold field emission of electrons; Fowler–Nordheim law; current–voltage characteristic (CVC); pointed cathodes; negative differential conductivity; van Hove singularity; superlattice

Citation: von Gratowski, S.V.; Kosakovskaya, Z.Y.; Koledov, V.V.; Shavrov, V.G.; Smolovich, A.M.; Orlov, A.P.; Denisjuk, R.N.; Wang, C.; Liang, J. Structural Inhomogeneities and Nonlinear Phenomena in Charge Transfer under Cold Field Emission in Individual Closed Carbon Nanotubes. *Micro* **2023**, *3*, 941–954. https://doi.org/10.3390/micro3040064

Academic Editor: Hiroshi Furuta

Received: 14 June 2023
Revised: 20 October 2023
Accepted: 24 October 2023
Published: 5 December 2023

1. Introduction

Experimentally, carbon nanotubes (CNTs) were discovered in 1991 by Iijima [1] and almost simultaneously and independently in [2,3]. First, CNTs were discovered as multi-walled carbon nanotubes (MWCNTs). The existence of single-walled carbon nanotubes (SWCNTs) was experimentally proved in 1993 [4,5]. Cold field emission (CFE) from carbon nanotubes was discovered in [6] and after this was extensively studied, see, for example, reviews [7,8] and the literature cited therein. The CFE phenomenon is very interesting from the viewpoint of fundamental science and consistently attracts the interest of researchers [6–11]. CFE from CNTs makes it possible to study the features of the work function and transport under field emission conditions for individual 1D objects and their arrays. Individual CNTs are actually large single molecules, which demonstrate field emission in the case of ballistic transport [12,13]; see the review [14] and the literature cited therein.

CFE from CNTs is also of great practical interest, since high-efficiency cathodes can be created on the basis of CNTs, which open up the possibility of developing a new generation of microwave and THz components for micro- and nano-solid state and vacuum electronics, including generators, detectors, etc. [7,8,14–20]. The emission of single electrons from individual CNTs makes it possible to create single-electron devices, which are necessary for quantum technologies [21–23]. Miniature X-ray sources based on CNTs have also been created [7,8,23–26].

Cathodoluminescence from CNTs in the optical range was observed in [27]. On the basis of cathodoluminescence, it is possible to create both conventional light sources and flexible screens. It is also suggested [28–32] that CNT-based probes for different scanning microscopes such as atomic force (AFM) [28] make it possible to create scanning tunneling microscopes (STMs) [29–31]. Due to the high density of the emission current and the small size of the emission region, these microscopes can increase the spatial resolution and image brightness. The CNT size makes it possible to scan by AFM deep and narrow depressions on the sample surface, which is impossible for conventional probes [28,29]. The next application is vacuum meters based on CNTs [33].

The CFE performance of a single isolated CNT can be evaluated as remarkable. This is due to the structural integrity, high thermal conductivity, and geometry of CNTs. It should be noted that it is possible in principle to miniaturize all devices based on cold field emission using CNTs. Many advantages of CNT-based cathodes are due to the high aspect ratio of CNTs; hence, the electric field strength in the vicinity of the CNT tip can be hundreds of times higher than the volume-average electric field strength generated by an external source. Another important advantage of CNTs is their chemical inertness and high mechanical strength. CNT-based cathodes have high efficiency, including energy efficiency and short turn-on time. However, field cathodes based on CNTs also have a number of disadvantages, the main of which being their fragility. The first studies of field emission from CNTs showed anomalously low voltages at which field emission is observed [6–8]. Despite great interest and numerous studies, there is still no complete understanding of the mechanism of cold field emission from CNTs. The emission currents were one or two orders of magnitude higher than it follows from the Fowler–Nordheim (F-NT) equation [34–40]. The main theory of CFE from CNTs, as well as field emission from the metals, is the Fowler–Nordheim theory, which was developed for bulk metal cathodes [22] and its various modifications [7,8,35–38].

Thus, the fundamental question of the nature of field emission from CNTs remains relevant, without solving which it is hardly possible to select the optimal structure and further develop cathodes and other devices from CNT. Most of the articles devoted to CFE from CNTs explain the effect of anomalously low voltages at which it is observed on the basis of various modifications of the Fowler–Nordheim theory. In order to explain the discrepancy between the experimental data and these theories, special coefficients are often introduced using the β-factor associated with the microgeometry of CNTs [7,8]. At the same time, there are other theories, alternative to the Fowler–Nordheim theory, which are confirmed experimentally; moreover, they explain many new effects in CNTs observed in the cold field emission mode. Among such theories, we should mention the studies [41–44] in which a theory was put forward according to which the mechanism of cold field emission from CNTs is explained on the basis of resonance tunneling of electrons from the near-surface region of the cathode due to size quantization. Such a resonance occurs when the Fermi level coincides with the size quantization level of a CNT [44]. It is shown in these papers that in the case of resonant scattering, the transmission coefficient can be significantly higher and, in the limit without a reflective potential, close to unity, which significantly reduces the cold field emission threshold. Also noteworthy are the works [45,46], which offer an explanation of the cold field emission mechanism based on the Coulomb blockade. Experimentally, the Coulomb blockade manifests itself in the steps in the I –V characteristics. In most of experimental works confirming the theory of Fowler–Nordheim, the I–V characteristics were measured for large gaps between the CNT and the anode (tens of microns). With such gaps, the onset of cold field emission is observed when a voltage of several hundred volts is applied. Accordingly, the voltage sweep when measuring the I-V characteristic is completed with steps of several tens of volts

(>30 V) [47]. Under such experimental conditions, the I-V characteristics are satisfactorily approximated by the Fowler–Nordheim function. At the same time, there are works in which the I-V characteristics were measured at small gaps between the CNT emitter and the anode (hundreds of nanometers). Naturally, to exclude the possibility of breakdown, the applied voltages were tens of volts, and the I-V characteristic sweep was made in steps of several tens of millivolts; see, for example, [48,49]. In these works, only the general character of the I-V characteristic envelope is well approximated in Fowler–Nordheim coordinates; however, peak-like features are observed in the I-V characteristic. When measuring the I-V characteristics with a voltage sweep in steps of several tens of volts, these features may simply remain unnoticed, in particular, due to a too large sweep step. Thus, further refinement of the nature of I-V characteristics is necessary to elucidate the mechanism of cold field emission from CNTs.

In this regard, in the present work, we measured the I-V characteristic in the cold field emission mode for single CNTs at small gaps between the anode and CNT. The I-V measurements were carried out at a voltage sweep with a step of 20–30 mV. In this mode, it is possible to detect details of the I-V characteristics that would not be noticed in studies with a large step. The present studies were carried out on closed single CNTs in order to exclude the influence of CNTs on each other and the collective effects of many CNTs. The resonance peaks found in the present work are explained using a model involving Van Hove singularities.

2. Materials and Methods

The synthesis of CNT arrays was carried out by electron-beam evaporation of high-purity 99.99% reactor graphite in a vacuum of 10^{-5} Torr at room temperature on a substrate. The arrays of CNTs obtained by this procedure were the result of deposition of carbon atoms on the surface of the substrates. The substrates were mirror polished silicon, quartz, anodized aluminum, graphite, and ceramics. The CNT layers deposited on a silicon substrate are a mixture of multiwalled CNTs with a diameter of 3 to 5 nm and single-walled CNTs with a diameter close to 1.1 nm. Layers deposited on a quartz substrate consist mainly of single-walled CNTs with a diameter close to 1 nm. The procedure of synthesis was described for the first time in [2,6]. Individual CNTs were fabricated by the discharge-arc method by depositing carbon on wire electrodes made of tungsten, nickel, and platinum. The discharge-arc method is based on the thermal sputtering of a graphite anode in an arc discharge plasma burning in a helium atmosphere. The sputter products are deposited on the chamber walls and on the cathode surface (up to 90%). A single CNT synthesized by the arc method was fixed on the top of a needle-shaped volumetric cathode made of tungsten or steel, which, in turn, was attached to the microscope stage with conductive paste.

Microscopy Measurements Methods

The AFM measurements were carried out using a "Nanoscan" scanning probe microscope. A piezoceramic resonator with high bending stiffness of the cantilever k $\approx$ 104–105 N/m and a resonant frequency f_0 of about 12 kHz was used as a probe. A trihedral diamond pyramid with an apex angle of about 60° was used as a needle; the effective rounding radius of the tip of the needle was about 100 nm. A needle with a sufficiently large radius of curvature was chosen, which made it possible to measure precisely the macroscopic characteristics of the sample with averaging over a region of the order of tens of nanometers. The study of SEM images was carried out using a 1540 XB Crossbeam Neon40EsB SEM, Carl Zeiss, Jena, Germany. All SEM images were taken at an accelerating voltage of 20 kV using a secondary electron detector. STM images were obtained using a Scan-8 scanning tunneling microscope in two modes: (a) in the dI/dZ regime, by changing the tunneling current; in this geometry, the sample was located in the X, Y-plane, with $U_{const} = 0.27$ V, and a step size of 0.1 nm, and (b) in the I regime, with $I_{const} = 500.0$ PA, with a step size of 0.8 nm.

Experimental studies of the charge transfer features were performed on the circuit of a nanotube emitter. The diode cell for measuring the emission characteristics of CNTs was assembled in a NEON 49 Carls Zeiss scanning electron microscope. This SEM is additionally equipped with an ion microscope column and Kleindiek micromanipulators with electrodes as well as two SE-2 optical sensors with a spectral range from 1720 to 760 nm. The cathode emitters for the experiments were various single CNTs with diameters from 2 to 14 nm and a length of about 1 µm. The acicular bulk conductive cathode, in turn, was attached to the SEM table with a conductive paste. A pointed tungsten electrode manipulator of a microscope with a diameter of $\sim$ 0.5 mm sharpened to 100–200 nm served as the anode. The use of a micromanipulator made it possible to set the gap between the tungsten anode and the tip of the CNT emitter in the range from several hundred nm to 1 µm. The scheme for measuring the current–voltage characteristics (I-V characteristic) of nanodiodes is shown in Figure 1. This scheme makes it possible to reverse the signs on the electrodes and carry out measurements in the voltage sweep mode with a step of 0.02 V. In order to avoid a short circuit in the microscope chamber and heating of the electrodes, the scheme provided a voltage and a current limit. At micron gaps between the electrodes, the voltage did not exceed 30 V. At gaps of several tens of microns, the voltage could be increased to 200 V. In any case, the current did not exceed 1 µA. If it was necessary, a current sweep could be carried out. The measured values of voltage and current were displayed on the screen in the form of I-V characteristics. Thus, we were able to track the change in the current and voltage between the CNT and the opposite electrode and, simultaneously, to observe all the changes occurring in the diode system by the SEM. Electron-microscopic control of the electrode with CNTs and the opposite tungsten electrode was carried out before and after the measurement of the I-V characteristics.

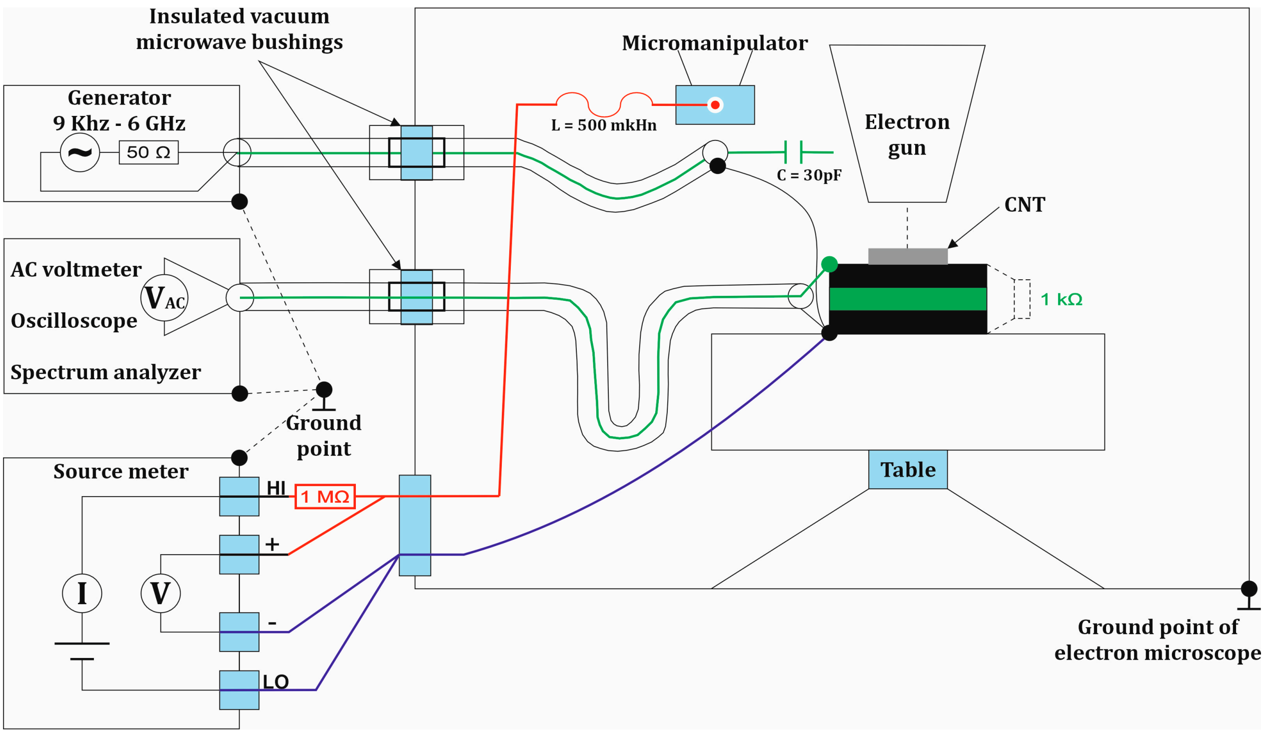

Figure 1. Scheme of measurements of the I-V characteristics of nanodiode samples based on CNTs in the SEM chamber.

The measurements of I-V characteristics in an electrostatic field were carried out with a voltage sweep with a step of 30 mV, which was set by a highly stable programmable Keithley 2400 source with an error of at most + 5 µV. The measurements of the direct emission current and voltage in the emitter circuit were carried out with an error of +10 PA and 1 µV, respectively.

3. Experimental Results

3.1. Experimental Studies of the Structure of CNTs

SEM micrographs of a diode section with single CNTs are shown in Figure 2a, and those of the array of CNTs are shown in Figure 2b. The structure of the samples of closed CNTs was studied by various microscopes—atomic force microscope (AFM), SEM, and STM. The study of the structure of the CNTs by all microscopes shows that the CNTs are closed; see also [2,6].

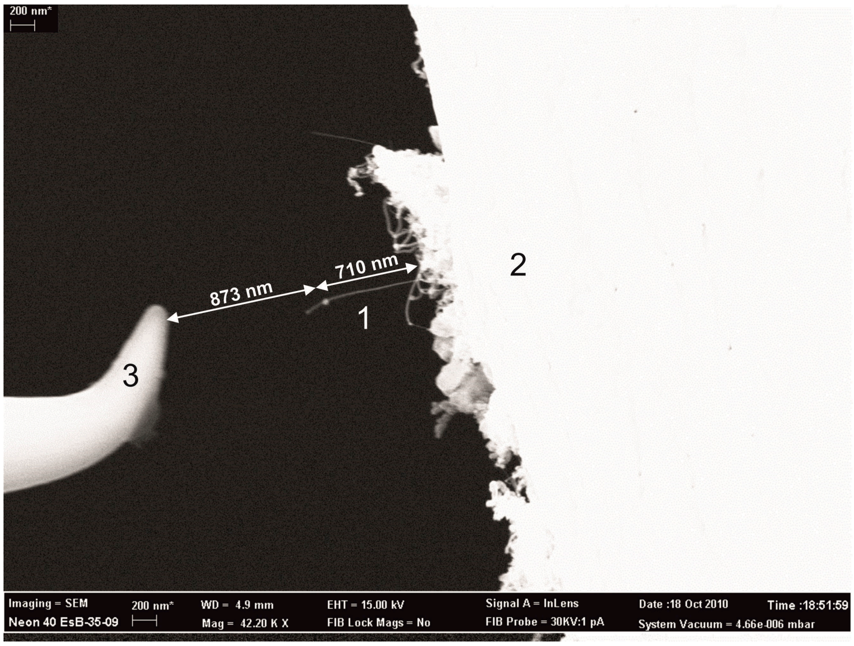

(**a**)

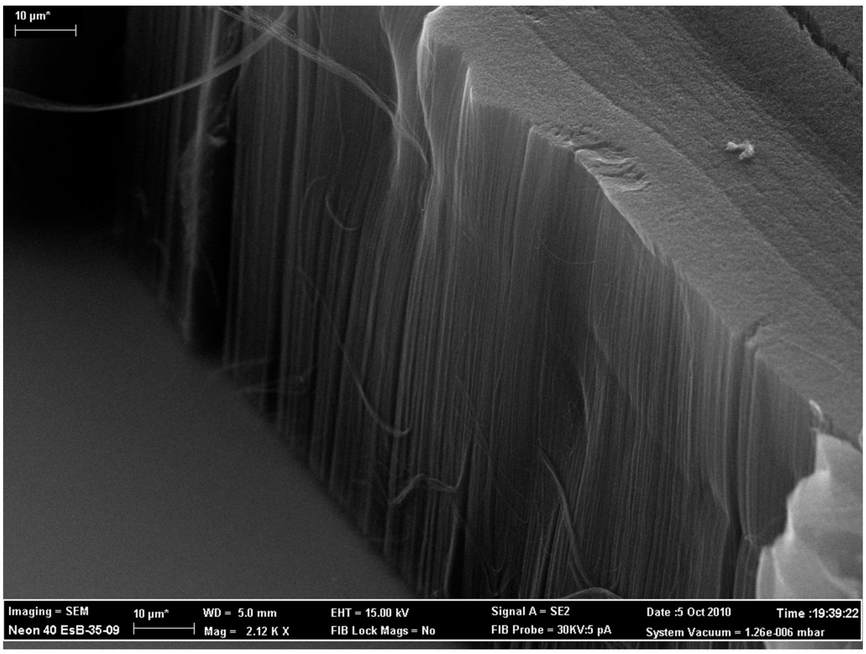

(**b**)

Figure 2. The samples of CNTs studied in SEM. (**a**) SEM image of the single CNT in the scheme for measuring its current–voltage characteristic (I-V characteristics) on a nanodiode mock-up. 1—nanotube emitter, 2—cathode, 3—tungsten microwire anode. The CNT length is 710 nm; the distance to the anode is 873 nm. (**b**) The array of the oriented CNTs.

Micrographs of diode structures of closed CNTs were obtained by AFM, SEM, and STM on the diode circuit with the CNT cathode, anode, and vacuum gap in the cold field emission mode (CFE). Structural inhomogeneities in closed CNTs were studied in situ under conditions of CFE for the diode scheme shown in Figures 3–6.

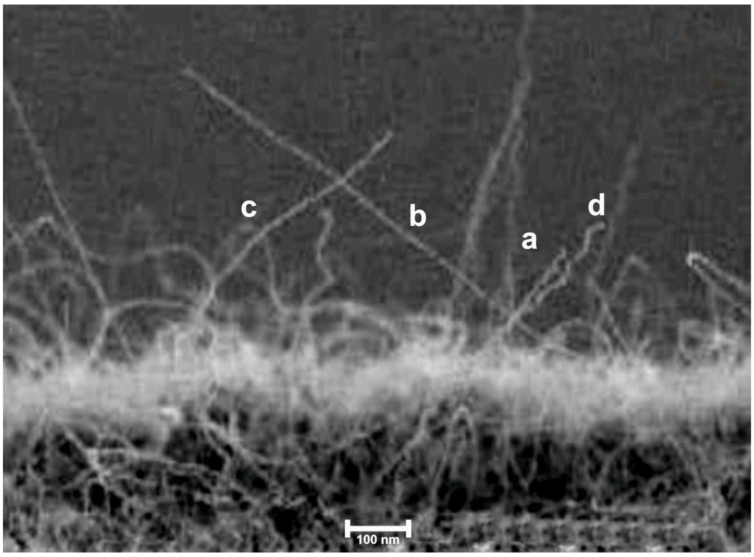

Figure 3. Micrographs of CNT samples obtained in SEM. An SEM image of CNTs that have different types of large-scale lattice deformations defined with the letters "a", "b", "c", and "d" on the figure.

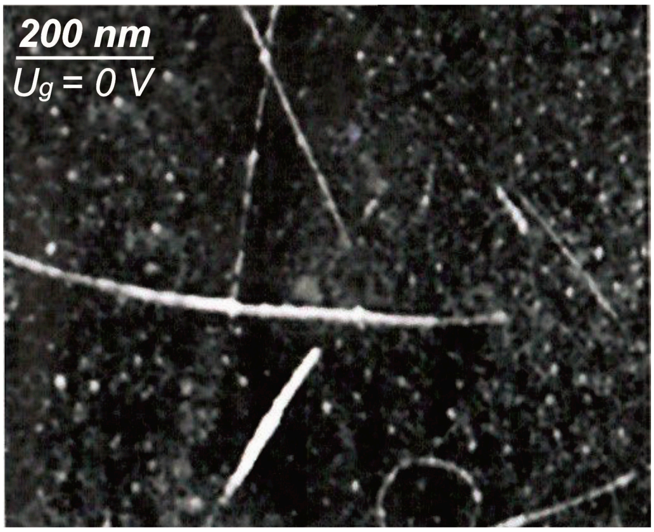

Figure 4. AFM image of CNT superlattices obtained at external electric field $U_g = 0$.

Figure 3 shows SEM micrographs of CNT samples with different types of lattice deformations, which are indicated by letters "a", "b", "c", and "d".

Figure 4 shows the AFM image of CNT superlattices at $U_g = 0$. Figure 5 shows mi-crographs of the superlattices detected in single CNTs in SEM (5a), AFM (5b) and STM (5c) images. During this study of micrographs in Figure 5a,b and Figure 6, the external field was directed along the CNT, and in Figure 5c, the external field was directed across it.

The superlattice shown in Figure 5a revealed a period of about 30–40 nm. In Figure 5b, one can see the AFM image of a CNT superlattice (period of ~30–40 nm). The emission current also flows along the CNT. Figure 5c shows the STM micrograph of a superlattice in CNTs with a period of about 3 nm. The applied electric field is perpendicular to the CNT axis. Figure 6 shows an SEM image of a nanodiode in secondary electrons of CNTs with a superlattice with a period of ~30–40 nm.

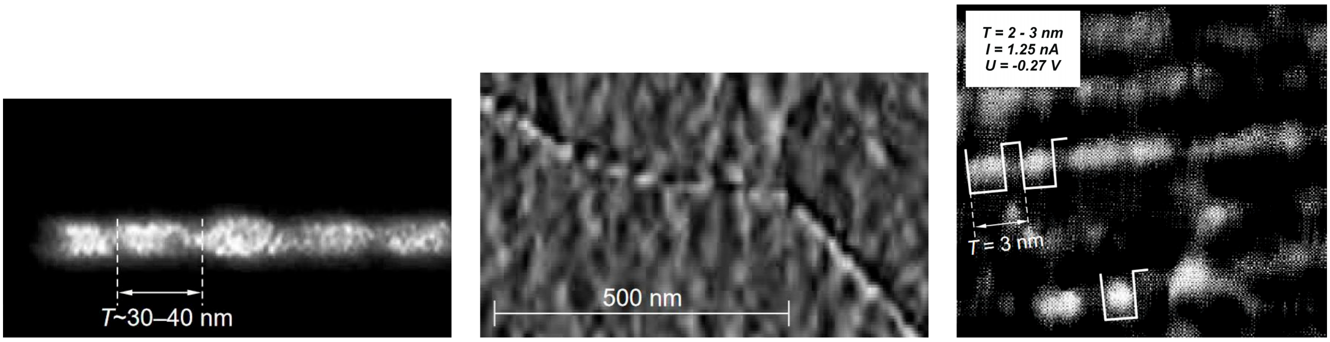

(**a**) (**b**) (**c**)

Figure 5. Study of superlattices detected in single CNTs in SEM, AFM and STM. (**a**) Superlattice revealed in SEM image, period about 30–40 nm. The emission current flows along the CNT. (**b**) AFM image of a CNT superlattice (period $\sim$ 30–40 nm). The emission current flows along the CNT. (**c**) STM micrograph of a superlattice in CNTs (period T~3 nm). The applied electric field is perpendicular to the CNT axis. Current $I = 1.25$ nA, $U = 0.27$ V.

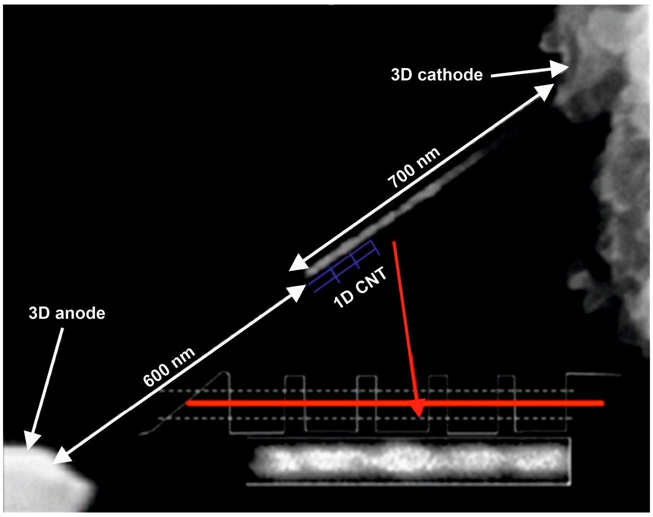

Figure 6. SEM image of a nanodiode in secondary electrons.

3.2. Experimental Studies of the Features of Charge Transfer in the Circuit of a Nanotube Emitter

Figure 7 shows an example of the SEM image of one of the diode structures with a single CNT deposited on a tungsten electrode.

The CNT length was approximately 700 nm. In the experiments, the CNT diameter was about 14 nm. The distance between the tip of the nanotube and the tungsten counter electrode was at least 0.5 μm. Figure 8a,b show some of the obtained I-V characteristics. Figure 8a shows the I-V characteristic plotted in I-V coordinates, and Figure 8b shows the I-V characteristic plotted in $\log(I/U^2) - 1/U$ coordinates or Fowler–Nordheim coordinates. The dotted line is a straight line corresponding to the Fowler–Nordheim function. Based on these experimental data, we estimated the electron work function φ and the electric field gain at the tip of the free end of the nanotube β. The threshold voltage of the beginning of the emission V_{thr} obtained from Figure 8b is 1.079 V. The parameter (R^2) for fitting to the Fowler–Nordheim function in Figure 8 is about 0.47.

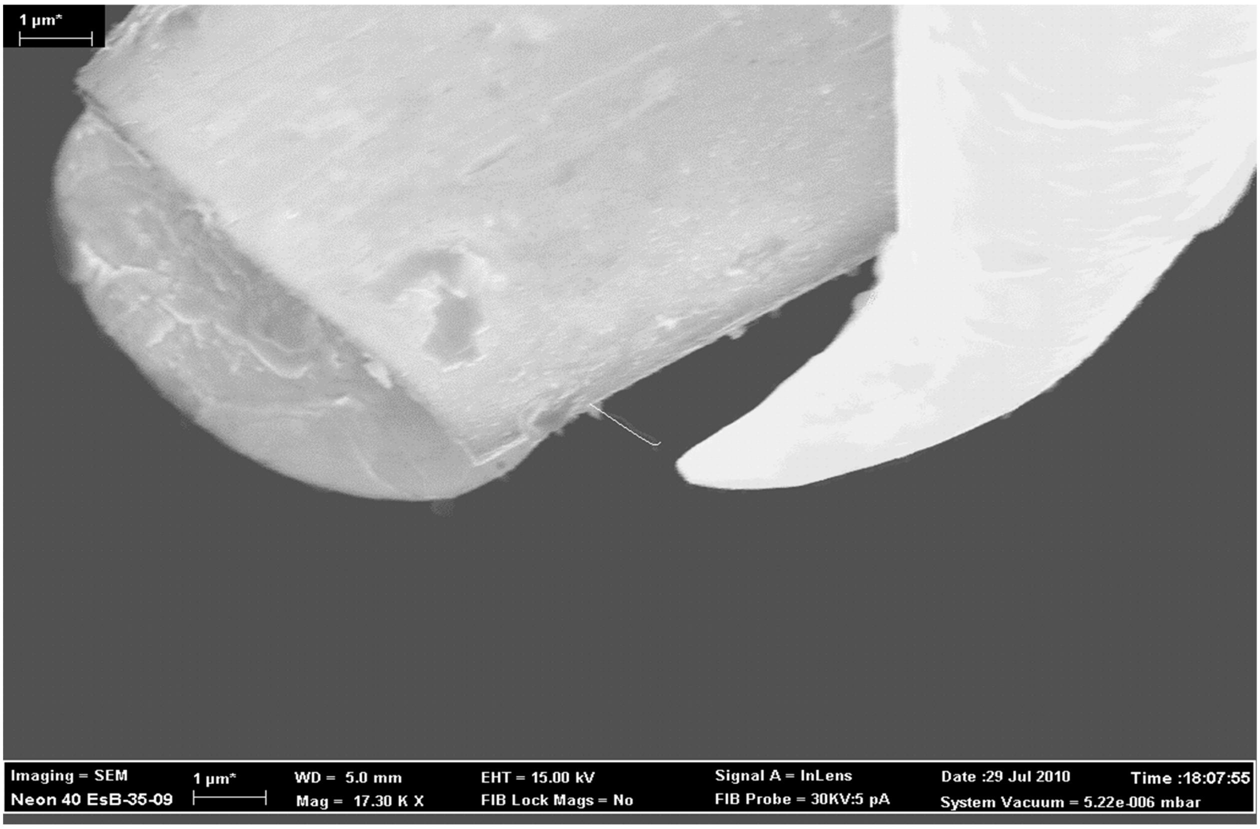

Figure 7. SEM micrograph showing a diode structure, one of the electrodes of which is a single CNT deposited on a tungsten electrode.

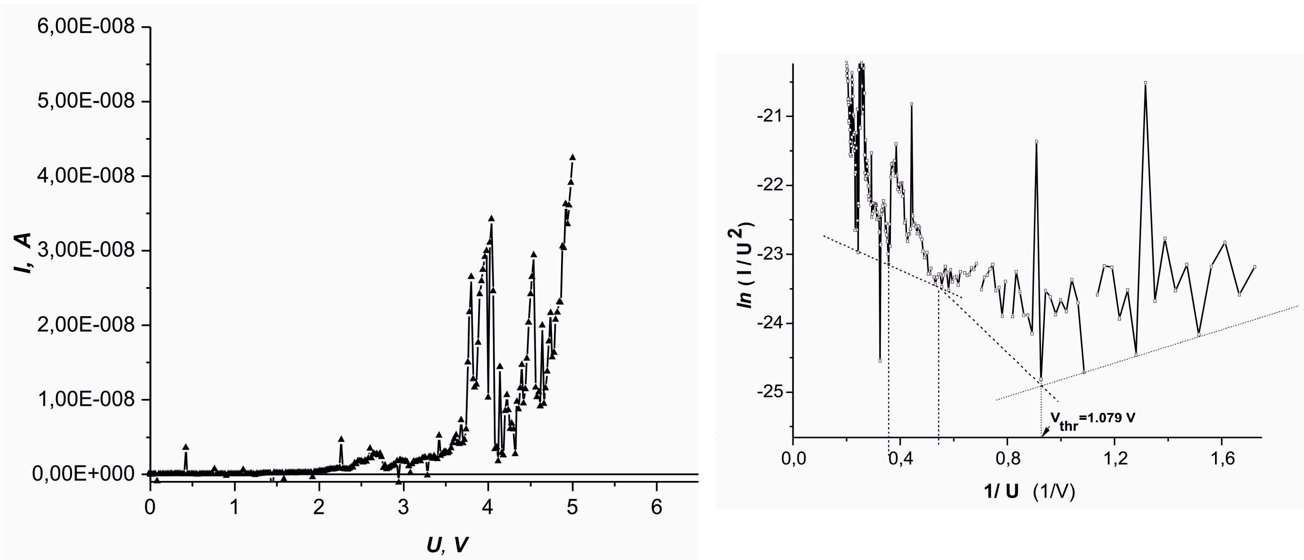

(**a**) (**b**)

Figure 8. I-V characteristic of the field emission measured on the nanodiode model (**a**) and the corresponding graph plotted in $\log(I/U^2) - 1/U$ coordinates (**b**). The dotted line is a straight line corresponding to the Fowler–Nordheim function. V threshold is 1079 V_{thr}.

4. Discussion

Superlattices in CNTs have been theoretically and experimentally considered in many works, for example, [50–53]. In [50], the elastic free energy of CNTs grown by the iron-catalyzed decomposition of acetylene was theoretically considered to provide the equilibrium shape of slightly curved CNTs. Equilibrium forms have been found for both stable and metastable cases. All of the found equilibrium forms are deformation superlattices, which were observed in the experiments of the authors of [50]. As suggested in this work, the deformations are caused by fluctuations in the growth conditions, such as pressure, temperature, and vapor composition. Also in our experiments, the results clearly show the presence of deformations along the CNT length. See Figure 3, which could also be caused by growth conditions. Superlattices in an electric field perpendicular to the CNT axis were theoretically considered in [51]. In this paper, the motion of an electron in a CNT carbon nanotube (n, 1) is considered as a de Broglie wave propagating along a helix on the nanotube wall. It is theoretically shown that this motion leads to periodicity of the electron potential energy in the presence of an electric field normal to the nanotube axis; the period of this potential is proportional to the nanotube radius and greater than the interatomic distance in the nanotube. As a result, the behavior of an electron in an (n, 1) nanotube in a transverse electric field is similar to a semiconductor superlattice. That is, in this case, the size of the superlattice inhomogeneities observed in our experiments in a field perpendicular to the CNT axis coincides in order of magnitude with the inhomogeneities observed in our experiments.

Figure 8a,b shows the CNT's I-V characteristics in the course of the cold field emission. It has been established that the voltage has thresholds, and resonant peaks are observed on the I-V characteristic. In the region of peaks, the emission current exceeds by one to three orders of magnitude the calculated one using the Fowler–Nordheim (F-N) function, and there are also smaller peaks. The I-V characteristics with resonance peaks are not rectified in F-N coordinates. In general, the I-V has nonlinear characteristics. The graphs clearly show the absence of the current saturation in the measurement region. The width of the resonant peaks increases with increasing the applied voltage from several tens of millivolts to tens of volts. Figure 8b shows the I-V characteristics in Fowler–Nordheim coordinates, and the threshold of the beginning of emission U_{thr} is clearly visible and $U_{thr} = 1079$. It is noted that the voltage sweep step is of decisive importance for the detection of I-V characteristics peaks. Thus, at a voltage sweep step of several millivolts, the first resonance peak, the threshold for the onset of emission, was observed at a field strength between the anode and cathode of the order of 1 V/µm.

When the step was increased by an order of magnitude, the U_{thr} threshold was in the region of 10 V/µm. However, there have been cases where U_{thr} was as low as 0.36 V, which is many times lower than the work function measured by the photoelectric effect.

On the I-V characteristics with peaks, regions of negative differential conductivity (NDC) are clearly visible. Thus, from the above I-V characteristics and its comparison with the Fowler–Nordheim model, it can be seen that in the regions of high and low currents, there are significant deviations from the theory in the framework of the Fowler–Nordheim model.

In [51,54–56], taking into account the quantum nature of the electron spectrum and high aspect ratio, it was shown that the emission current $j_{1D}(E)$ from a one-dimensional emitter CNT through a potential barrier into vacuum is described by the following equation:

$$j_{1D} = \frac{2e_0}{h^3} \sum_{n=1,\,2\ldots} * \sum_{m=1,2\ldots} * \int_{p_x=0}^{p_{x,\,m,\,n}} N(\varepsilon) D(\varepsilon_x) \frac{\partial \varepsilon}{\partial p_x} dp, \tag{1}$$

where

$$N(\varepsilon)_\alpha \frac{\vartheta(\varepsilon - \varepsilon_{Fm,n})}{\sqrt{\varepsilon - \varepsilon_{Fm,n}}};$$

Here, $N(\varepsilon)$ is the CNT electron density depending on electron current energy ε related to the momentum component p along the nanotube X axis, Θ is the Heaviside function, which is equal to Θ for $x > 0$ and $\Theta = 0$ for $x < 0$, $D(\varepsilon,\ x)$ is the potential barrier transparency, h is Planck's constant, e_0 is the electron charge, $\varepsilon_{m,n}$ are the energies corresponding to band breaks near Van Hove energy singularities, and $m,\ n$ are integer sub-band numbers corresponding to Van Hove singularities.

The appearance of van Hove singularities in CNTs was first experimentally shown in [54] and then in other works [55,56]. Since there are Van Hove singularities at energies corresponding to the quantum levels of CNTs, this property manifests itself as resonant conductivity peaks in the I-V characteristics, and in the F-N coordinates $(\ln(j/U_2) - 1/U)$ the I-V characteristic will be a straight line with a kink at the Van Hove points. According to [54,55], the observed peaks may correspond to the features of the density of states at Van Hove energies for CNTs. The graphs show significant deviations from linearity and the absence of current saturation, which indicates a fundamentally different field emission mechanism than F-NT.

Cold field emission from CNTs can be significantly affected by periodic inhomogeneities in the structure of CNTs, including superlattices. The appearance of a periodic superlattice in the case of one-dimensional systems leads to the splitting of the energy bands into a set of sub-bands [57,58], and energy gaps are opened at the center and at the edges of the Brillouin zone, which can have a significant effect on the CFE. In general, the emergence of periodic inhomogeneities, primarily superlattices, can play a significant role in the features of many CNT properties, including the transport properties and the mechanism of cold field emission. There are not only large peaks but also small peaks in the I-V characteristics, which create sub-bands in the band structure of CNT, and these sub-bands due to the same mechanism cause smaller Van Hove singularities and smaller amplitude peaks.

Superlattices arising in nanowires and nanotubes attract significant attention from scientists, see, for example, [59] and the literature cited therein. It should be noted that there is a fundamental difference between superlattices purposefully created during the synthesis of nanowires and nanotubes, which are discussed in the cited work, and superlattices that arise as a result of structural transformation in nanowires and nanotubes, which were grown as homogeneous nano-objects.

For the first time, superlattices were experimentally discovered and theoretically predicted in [50], where it was found that a modulated equilibrium or quasi-equilibrium form of CNTs grown by the iron-catalyzed decomposition of acetylene can have various deformations, which are superlattices. That is, superlattices have also been found in the studied closed CNTs grown in a different way but also with existing deformations.

In these works, as well as in [60], superlattices were observed along the CNT axis. The appearance of superlattices in a field perpendicular to the CNT axis was theoretically predicted in [51]. Later, superlattices in CNTs were experimentally observed by SEM in [61] and also in the works by the same group of authors [62–64]. The authors of [61–64] associate such superlattices with ordered associates of CNTs. According to the authors of [61–64], this can lead to a significant change in the electronic structure of weakly interacting CNTs that form a regular associate. According to these works, such effects can be understood if we take into account that all electronic states in an ensemble of parallel interacting CNTs are collectivized. With respect to different tubes, the electronic wave functions have the form of standing waves, whose distributions of nodes and antinodes correspond to the brightness distributions of images of individual CNTs. Hence, it follows that even in the case of sufficiently weak exchange bonds between individual CNTs, their electronic structure can undergo qualitative changes. For example, in an ensemble of metallic CNTs, some of them can acquire semiconductor properties [63]. Also, the appearance of superlattices in CNTs was theoretically considered in [51,52,58].

The experimental results of the present work confirm the observation of superlattices in CNTs. It should be noted that the data on superlattices obtained here were performed for a nanodiode structure with CNTs consisting of a cathode with CNTs, an anode, and a vacuum gap: that is, in a different scheme than in the works cited above. This may indicate the possible universality of superlattices in CNTs.

The appearance of peaks in the I-V characteristics in cold field emission mode with CNTs as emitters was also found in [48,49] at small distances between a CNT and cathode in [23,48,49] and in [64,65] at larger distances between a CNT and cathode.

5. Conclusions

The experimental data obtained testify to the observation of anomalies in the form of peaks on the I-V characteristic of cold field emission in closed CNTs with the appearance of negative differential conductivity at low and high currents and a significant deviation both from the linearity of the I-V characteristic and from the Fowler–Nordheim law. Also, it is found that there is no current saturation. The observed peaks, as the authors suggest, are associated singularities in the density of electronic states of CNTs near the Van Hove energies of CNTs. Negative differential conductivity near these peaks can be a promising basis for creating microwave generators based on cold field emission from CNTs. On the basis of cold field emission from CNTs, it is possible to create microdevices, such as vacuum microtube sources, microtriodes and many other microdevices for the components for new generations of quantum vacuum microelectronics [66,67]. On the other hand, cold field emission from single CNTs can make it possible to create single nanodevices, for example, individual nanodevices for single electronics, sub-10 nm electron beam lithography, and atomic resolution electron microscopy [23].

Finally, two types of superlattices were found in closed CNTs under conditions of cold field emission. First, there is a large-scale one, which occurs when current flows along the axis of the CNT; this superlattice is presumably caused by the periodic deformation of CNT walls and has a characteristic period of approximately 30–40 nm. Second, there is a small-scale superlattice with a characteristic period on the order of 2–3 nm, which appears when the field is applied perpendicular to the CNT axis. The discovered superlattices can influence the mechanisms of cold field emission in closed CNTs and the deviations from the Fowler–Nordheim law in closed CNTs. Further studies are needed to fully understand the mechanisms of the emerging structural inhomogeneities.

Author Contributions: S.V.v.G.—conceptualisation, writing—original draft, editing, Investigation, funding acquisition, methodology, project administration, supervision, validation, writing—review & editing, Z.Y.K.—conceptualisation, writing—original draft, experiments, investigation, methodology, resources, validation, V.V.K.—conceptualisation, writing—original draft, editing, validation, writing—review & editing, V.G.S.—conceptualisation, writing—review & editing, A.M.S.—experiments, investigation, A.P.O.—experiments, investigation, R.N.D.—data curation, writing—review & editing, C.W.—experiments, investigation, J.L.—experiments, investigation. All authors have read and agreed to the published version of the manuscript.

Funding: The work was supported by RSF, grant No 22-19-00783.

Data Availability Statement: The data is contained in the article.

Conflicts of Interest: The authors declare no conflict of interest.

References

1. Iijima, S. Helical microtubules of graphitic carbon. *Nature* **1991**, *354*, 56–58. [CrossRef]
2. Kosakovskaya, Z.Y.; Chernozatonsky, L.A.; Fedorov, E.A. Nanofiber carbon structure. *JETP Lett.* **1992**, *56*, 26.
3. Chernozatonskii, L.A. Barrelenes/tubelenes—A new class of cage carbon molecules and its solids. *Phys. Lett. A* **1992**, *166*, 55–60. [CrossRef]
4. Bethune, D.S.; Kiang, C.H.; de Vries, M.S.; Gorman, G.; Savoy, R.; Vazquez, J.; Beyers, R. Cobalt-catalysed growth of carbon nanotubes with single-atomic-layer walls. *Nature* **1993**, *363*, 605–607. [CrossRef]
5. Iijima, S.; Ichihashi, T. Single-shell carbon nanotubes of 1-nm diameter. *Nature* **1993**, *363*, 603–605. [CrossRef]
6. Chernozatonskii, L.A.; Gulyaev, Y.V.; Kosakovskaja, Z.J.; Sinitsyn, N.I.; Torgashov, G.V.; Zakharchenko, Y.F.; Fedorov, E.A.; Val'chuk, V.P. Electron field emission from nanofilament carbon films. *Chem. Phys. Lett.* **1995**, *233*, 63–68. [CrossRef]

7. Eletskii, A.V. Electron field emitters based on carbon nanotubes. *Uspekhi Fiz. Nauk* **2010**, *180*, 897–930. [CrossRef]
8. Eidelman, E.D.; Arkhipov, A.V. Field emission from carbon nanostructures: Models and experiment. *Phys.-Uspekhi* **2020**, *63*, 648. [CrossRef]
9. Cheng, Y.; Zhou, O. Electron field emission from carbon nanotubes. *Comptes Rendus Phys.* **2003**, *4*, 1021–1033. [CrossRef]
10. Milne, W.I.; Teo, K.B.K.; Mann, M.; Bu, I.Y.Y.; Amaratunga, G.A.J.; de Jonge, N.; Allioux, M.; Oostveen, J.T.; Legagneux, P.; Minoux, E.; et al. Carbon nanotubes as electron sources. *Phys. Status Solidi A* **2006**, *203*, 1058–1063. [CrossRef]
11. Lee, H.R.; Hwang, O.J.; Cho, B.; Park, K.C. Scanning electron imaging with vertically aligned carbon nanotube (CNT) based cold cathode electron beam (C-beam). *Vacuum* **2020**, *182*, 109696. [CrossRef]
12. Wu, Z.; Xing, Y.; Ren, W.; Wang, Y.; Guo, H. Ballistic transport in bent-shaped carbon nanotubes. *Carbon* **2019**, *149*, 364–369. [CrossRef]
13. Li, H.; Lu, W.G.; Li, J.J.; Bai, X.D.; Gu, C.Z. Multichannel ballistic transport in multiwall carbon nanotubes. *Phys. Rev. Lett.* **2005**, *95*, 086601. [CrossRef] [PubMed]
14. Eletskii, A.V. Transport properties of carbon nanotubes. *Phys.-Uspekhi* **2009**, *52*, 209. [CrossRef]
15. Zu, Y.; Yuan, X.; Xu, X.; Cole, M.T.; Zhang, Y.; Li, H.; Yin, Y.; Wang, B.; Yan, Y. Design and simulation of a multi-sheet beam terahertz radiation source based on carbon-nanotube cold cathode. *Nanomaterials* **2019**, *9*, 1768. [CrossRef] [PubMed]
16. Milne, W.I.; Teo, K.B.K.; Amaratunga, G.A.J.; Legagneux, P.; Gangloff, L.; Schnell, J.-P.; Semet, V.; Binh, V.T.; Groening, O. Carbon nanotubes as field emission sources. *J. Mater. Chem.* **2004**, *14*, 933–943. [CrossRef]
17. Zou, R.; Hu, J.; Song, Y.; Wang, N.; Chen, H.; Chen, H.; Chen, Z. Carbon nanotubes as field emitter. *J. Nanosci. Nanotechnol.* **2010**, *10*, 7876–7896. [CrossRef]
18. Xu, X.; Yuan, X.; Chen, Q.; Cole, M.T.; Zhang, Y.; Xie, J.; Yin, Y.; Li, H.; Yan, Y. A low-voltage, premodulation terahertz oscillator based on a carbon nanotube cold cathode. *IEEE Trans. Electron Devices* **2020**, *67*, 1266–1269. [CrossRef]
19. Gu, Y.; Yuan, X.; Xu, X.; Cole, M.; Chen, Q.; Zhang, Y.; Wang, B.; Li, H.; Yin, Y.; Yan, Y. A high-current-density terahertz electron-optical system based on carbon nanotube cold cathode. *IEEE Trans. Electron Devices* **2020**, *67*, 5760–5765. [CrossRef]
20. Huo, C.; Liang, F.; Sun, A.B. Review on development of carbon nanotube field emission cathode for space propulsion systems. *High Volt.* **2020**, *5*, 409–415. [CrossRef]
21. Tang, Y.; Amlani, I.; Orlov, A.O.; Snider, G.L.; Fay, P.J. Operation of single-walled carbon nanotube as a radio-frequency single-electron transistor. *Nanotechnology* **2007**, *18*, 445203. [CrossRef]
22. Soldatov, E.S.; Kolesov, V.V. The single electronics: Past, present, future. *RENSIT* **2012**, *4*, 71–90e.
23. Wang, A.; Zhao, J.; Chen, K.; Li, Z.; Li, C.; Dai, Q. Ultra Coherent Single Electron Emission of Carbon Nanotubes. *Adv. Mater. Adv. Mater.* **2023**, *35*, 2300185. [CrossRef] [PubMed]
24. Sugie, H.; Tanemura, M.; Filip, V.; Iwata, K.; Takahashi, K.; Okuyama, F. Carbon nanotubes as electron source in an x-ray tube. *Appl. Phys. Lett.* **2001**, *78*, 2578–2580. [CrossRef]
25. Musatov, A.L.; Gulyaev, Y.V.; Izrael'yants, K.R.; Kukovitskii, E.F.; Kiselev, N.A.; Maslennikov, O.Y.; Guzilov, I.A.; Ormont, A.B.; Chirkova, E.G. A compact X-ray tube with a field emitter based on carbon nanotubes. *J. Commun. Technol. Electron.* **2007**, *52*, 714–716. [CrossRef]
26. Parmee, R.J.; Collins, C.M.; Milne, W.I.; Cole, M.T. X-ray generation using carbon nanotubes. *Nano Converg.* **2015**, *2*, 1. [CrossRef]
27. Psuja, P.; Hreniak, D.; Strek, W. The concept of a new simple low-voltage cathodoluminescence set-up with CNT field emission cathodes. In Proceedings of the Reliability, Packaging, Testing, and Characterization of MEMS/MOEMS and Nanodevices VIII, San Jose, CA, USA, 28–29 January 2009; Volume 7206, pp. 132–137.
28. Wilson, N.R.; Macpherson, J.V. Carbon nanotube tips for atomic force microscopy. *Nat. Nanotechnol.* **2009**, *4*, 483–491. [CrossRef]
29. Shingaya, Y.; Nakayama, T.; Aono, M. Carbon nanotube tip for scanning tunneling microscopy. *Phys. B Condens. Matter* **2002**, *323*, 153–155. [CrossRef]
30. Clauss, W. Scanning tunneling microscopy of carbon nanotubes. *Appl. Phys. A* **1999**, *69*, 275–281. [CrossRef]
31. Biró, L.P.; Thiry, P.A.; Lambin, P.; Journet, C.; Bernier, P.; Lucas, A.A. Influence of tunneling voltage on the imaging of carbon nanotube rafts by scanning tunneling microscopy. *Appl. Phys. Lett.* **1998**, *73*, 3680–3682. [CrossRef]
32. Dai, H.; Hafner, J.H.; Rinzler, A.G.; Colbert, D.T.; Smalley, R.E. Nanotubes as nanoprobes in scanning probe microscopy. *Nature* **1996**, *384*, 147–150. [CrossRef]
33. Kim, S.J. Vacuum gauges with emitters based on carbon nanotubes. *Tech. Phys. Lett.* **2005**, *31*, 597–599. [CrossRef]
34. Fowler, R.H.; Nordheim, L. Electron emission in intense electric fields. Proceedings of the Royal Society of London. *Ser. A Contain. Pap. A Math. Phys. Character* **1928**, *119*, 173–181.
35. Forbes, R.G. Field emission: New theory for the derivation of emission area from a Fowler–Nordheim plot. *J. Vac. Sci. Technol. B Microelectron. Nanometer Struct. Process. Meas. Phenom.* **1999**, *17*, 526–533. [CrossRef]
36. Liang, S.-D.; Chen, L. Generalized fowler-nordheim theory of field emission of carbon nanotubes. *Phys. Rev. Lett.* **2008**, *101*, 027602. [CrossRef]
37. Jensen, K.L. Electron emission theory and its application: Fowler–Nordheim equation and beyond. *J. Vac. Sci. Technol. B: Microelectron. Nanometer Struct. Process. Meas. Phenom.* **2003**, *21*, 1528–1544. [CrossRef]
38. Lepetit, B. Electronic field emission models beyond the Fowler-Nordheim one. *J. Appl. Phys.* **2017**, *122*, 215105. [CrossRef]
39. Vul', A.; Reich, K.; Eidelman, E.; Terranova, M.L.; Ciorba, A.; Orlanducci, S.; Sessa, V.; Rossi, M. A Model of Field Emission from Carbon Nanotubes Decorated by Nanodiamonds. *Adv. Sci. Lett.* **2010**, *3*, 110–116. [CrossRef]

40. Katkov, V.L.; Osipov, V.A. Energy distributions of field emitted electrons from carbon nanosheets: Manifestation of the quantum size effect. *JETP Lett.* **2009**, *90*, 278–283. [CrossRef]
41. Xie, S.S.; Li, W.Z.; Qian, L.X.; Chang, B.H.; Fu, C.S.; Zhao, R.A.; Zhou, W.Y.; Wang, G. Equilibrium shape equation and possible shapes of carbon nanotubes. *Phys. Rev. B* **1996**, *54*, 16436. [CrossRef]
42. Fursey, G.N. *Field Emission in Vacuum Micro-Electronics*; Kluwer Academic/Plenum Publishers: New York, NY, USA; Springer: Berlin/Heidelberg, Germany, 2005; p. 205.
43. Yafyasov, A.; Bogevolnov, V.; Fursey, G.; Pavlov, B.; Polyakov, M.; Ibragimov, A. Low-threshold emission from carbon nano-structures. *Ultramicroscopy* **2011**, *111*, 409–414. [CrossRef] [PubMed]
44. Yafyasov, A.; Bogevolnov, V.; Fursey, G.; Pavlov, B.; Polyakov, M.; Ibragimov, A.; Fursei, G.N.; Polyakov, M.A.; Kantonistov, A.A. Field and explosive emissions from graphene-like structures. *Tech. Phys.* **2013**, *58*, 845–851.
45. Kleshch, V.I.; Porshyn, V.; Serbun, P.; Orekhov, A.S.; Ismagilov, R.R.; Malykhin, S.A.; Eremina, V.A.; Obraztsov, P.A.; Obraztsova, E.D.; Lützenkirchen-Hecht, D. Coulomb blockade in field electron emission from carbon nanotubes. *Appl. Phys. Lett.* **2021**, *118*, 053101. [CrossRef]
46. Pascale-Hamri, A.; Perisanu, S.; Derouet, A.; Journet, C.; Vincent, P.; Ayari, A.; Purcell, S.T. Ultrashort single-wall carbon nanotubes reveal field-emission coulomb blockade and highest electron-source brightness. *Phys. Rev. Lett.* **2014**, *112*, 126805. [CrossRef] [PubMed]
47. Padya, B.; Ravi, M.; Jain, P. Growth and integration of aligned carbon nanotube-based field emission cathode for electron gun device-level fabrication. *Nano Trends* **2023**, *2*, 100009. [CrossRef]
48. DI Bartolomeo, A.; Scarfato, A.; Giubileo, F.; Bobba, F.; Biasiucci, M.; Cucolo, A.M.; Santucci, S.; Passacantando, M. A local field emission study of partially aligned carbon-nanotubes by atomic force microscope probe. *Carbon N. Y.* **2007**, *45*, 2957–2971. [CrossRef]
49. Giubileo, F.; Di Bartolomeo, A.; Scarfato, A.; Iemmo, L.; Bobba, F.; Passacantando, M.; Santucci, S.; Cucolo, A. Local probing of the field emission stability of vertically aligned multi-walled carbon nanotubes. *Carbon N. Y.* **2009**, *47*, 1074–1080. [CrossRef]
50. Kibis, O.V.; Parfitt, D.G.W.; Portnoi, M.E. Superlattice properties of carbon nanotubes in a transverse electric field. *Phys. Rev. B* **2005**, *71*, 035411. [CrossRef]
51. Ayuela, A.; Chico, L.; Jaskólski, W. Electronic band structure of carbon nanotube superlattices from first-principles calculations. *Phys. Rev. B* **2008**, *77*, 085435. [CrossRef]
52. Shokri, A.A.; Khoeini, F. Electron localization in superlattice-carbon nanotubes. *Eur. Phys. J. B* **2010**, *78*, 59–64. [CrossRef]
53. Wilder, J.W.; Venema, L.C.; Rinzler, A.G.; Smalley, R.E.; Dekker, C. Electronic structure of atomically resolved carbon nanotubes. *Nature* **1998**, *391*, 59–62. [CrossRef]
54. Zhang, J.; Liu, S.; Nshimiyimana, J.P.; Deng, Y.; Hu, X.; Chi, X.; Wu, P.; Liu, J.L.; Chu, W.; Sun, L. Observation of van Hove singularities and temperature dependence of electrical characteristics in suspended carbon nanotube Schottky barrier transistors. *Nano-Micro Lett.* **2018**, *10*, 25. [CrossRef] [PubMed]
55. Yang, Y.; Fedorov, G.; Shafranjuk, S.E.; Klapwijk, T.M.; Cooper, B.K.; Lewis, R.M.; Lobb, C.J.; Barbara, P. Electronic transport and possible superconductivity at van hove singularities in carbon nanotubes. *Nano Lett.* **2015**, *15*, 7859–7866. [CrossRef]
56. Jaskólski, W.; Stachow, A.; Chico, L. Band structure and quantum conductance of metallic carbon nanotube superlattices. *Acta Phys. Pol.-Ser. A Gen. Phys.* **2005**, *108*, 697–704. [CrossRef]
57. Kim, P.; Odom, T.W.; Huang, J.L.; Lieber, C.M. Electronic density of states of atomically resolved single-walled carbon nanotubes: Van Hove singularities and end states. *Phys. Rev. Lett.* **1999**, *82*, 1225. [CrossRef]
58. Lieber, C.M. Nanowire superlattices. *Nano Lett.* **2002**, *2*, 81–82. [CrossRef]
59. Lambin, P.; Loiseau, A.; Culot, C.; Biro, L.P. Structure of carbon nanotubes probed by local and global probes. *Carbon* **2002**, *40*, 1635–1648. [CrossRef]
60. Grishin, M.V.; Dadidchik, F.I.; Kovalevsky, S.A. Ordered adsorption of carbon nanotubes on pyrolytic graphite Surface. *X-Ray Synchrotron Neutron Res.* **2001**, *7*, 103. Available online: http://www.issp.ac.ru/journal/surface/2001/07-2001.htm?ysclid=lpr5mrjes71202709 (accessed on 14 July 2023). (In Russian).
61. Dalidchik, F.I.; Grishin, M.V.; Kovalevsky, S.A. Features of the electronic structure of interacting nanocarbon particles. *Microsyst. Eng.* **2004**, *7*, 29–33. Available online: https://elibrary.ru/download/elibrary_9497233_15437905.pdf (accessed on 14 July 2023). (In Russian).
62. Dalidchik, F.I.; Balashov, E.M.; Grishin, M.V. Scanning tunneling spectroscopy of interacting nanocarbon sp2 structures. *Russ. Chem. J.* **2005**, *159*, 98–104.
63. Dalidchik, F.I.; Shub, B.R. Scanning tunneling microscopy and spectroscopy of imperfect and interacting nanoparticles (metal oxides and carbon). *Russ. Nanotechnol.* **2006**, *1*, 82–96. (In Russian)
64. Bonard, J.M.; Dean, K.A.; Coll, B.F.; Klinke, C. Field emission of individual carbon nanotubes in the scanning electron microscope. *Phys. Rev. Lett.* **2002**, *89*, 197602. [CrossRef]
65. Bonard, J.M.; Salvetat, J.P.; Stöckli, T.; Forro, L.; Chatelain, A. Field emission from carbon nanotubes: Perspectives for applications and clues to the emission mechanism. *Appl. Phys. A* **1999**, *69*, 245–254. [CrossRef]

66. Bower, C.; Zhu, W.; Shalom, D.; Lopez, D.; Chen, L.H.; Gammel, P.L.; Jin, S. On-chip vacuum microtriode using carbon nanotube field emitters. *Appl. Phys. Lett.* **2002**, *80*, 3820–3822. [CrossRef]
67. Manohara, H.; Dang, W.L.; Siegel, P.H.; Hoenk, M.; Husain, A.; Scherer, A. Field emission testing of carbon nanotubes for THz frequency vacuum microtube sources. In Proceedings of the Reliability, Testing, and Characterization of MEMS/MOEMS III, San Jose, CA, USA, 27–29 January 2003; Volume 5343, pp. 227–234.